População estelar em galáxias: Métodos Síntese

Aula 2

1) Síntese utilizando estrelas estrelas + função de luminosidade
2) Síntese utilizando aglomerados estelares de diferentes idades e metalicidade

Aula 3

1) Identificação das linhas espectrais da galáxia selecionada para o trabalho de síntese
2) Índices de Lick (Faber et al. 1985 ApJ S 57 11)

A COMPARATIVE STUDY OF THE STELLAR CONTENT IN NORMAL AND ACTIVE NUCLEI OF SPIRAL GALAXIES

HORÁCIO A. DOTTORI and MIRIANI G. PASTORIZA

Instituto de Física, Universidade Federal do Rio Grande do Sul, Porto Alegre, Brasil

1986Ap&SS.121..147D

(Received 18 September, 1985)

Abstract. We present spectrophotometry and *UBV* photometry of the central region of spiral galaxies. The sample consists of the Seyfert galaxies NGC 1566, 3783 and IC 4329A; NGC 1097, 2997, and 5236 containing peculiar nucleus and NGC 5530, 5643, and 6699 with normal nucleus.

The stellar composition of the nuclei was derived by treating the equivalent widths of a sample of absorption lines with the method of constrained nonlinear optimization. The observed continua and the *UBV* colours were compared with the theoretical results in order to obtain the internal reddening and the contribution of the hot gas or non-thermal radiation. The age of the last cycle of star formation, the internal absorption and the theoretical relations M/L and H/K Ca II present differences among the three types of nuclei.

TABLE Ib

Equivalent width of the observed absorption lines. Measurements are quoted together with $\frac{1}{2}$ of the difference between the two observed spectra. A mean error can be obtained from the mean value of this deviation, and can be set between 15 and 30%.

λ [Å]	Line element	5530	5643	6699	2997	1097	5236	1566	3783	4329A
3632	Fe I	8.51							1.13	
		3.00							0.21	
3832	Mg I + Hg	6.37	3.83	11.55	2.23	7.61	1.25	1.25	4.20	
		0.60	0.07	0.35	1.10	0.01	0.05	0.05	1.12	
3854	Si II	8.83				0.39				
		2.40				0.30				
3889	H8 (+ Fe I)			3.66		4.59			0.30	
				0.70		0.10	3.11		0.46	
3933	K Ca II	11.86	2.56	12.16	4.32	7.20	0.10	3.11	5.65	2.0*
		3.00	1.50	0.80	0.30	0.30	1.51	0.10	0.98	
3970	Ca II + Hε	11.56	4.15	12.27	5.54	7.91	0.50	1.51	emiss.	
		2.00	1.70	2.40	1.50	1.00		0.50		
4101	Hδ	0.86			2.95	2.52				
		0.14			0.70	0.90	2.89			
4300	G band	4.78	4.30	2.00	3.14	5.70	0.10	2.89	2.69	4.60
		0.75	4.00	2.00	0.80	0.15		0.10		
4341	Hγ				1.22				emiss.	
					1.20					
4380	Fe I	3.76	1.25						0.53	
		0.25	1.00						0.55	
4440	Ca I + Fe I								0.45	4.17
									0.39	
4532	Fe I								0.74	
									0.88	
4592	Ca I + Fe I		3.40						0.50	
			3.00						0.87	
4658	C2 Swan band								1.30	4.86
									0.72	
4861	Hβ			4.42						
				0.20			1.06			
5174	Mg I	1.96	4.71			1.06	0.09	1.30	2.30	3.97
		0.50	0.74			0.09	1.01	0.30	1.22	
5270	Fe I (+ Ca I)	2.34	2.17	2.53	2.10	1.01	1.00		1.10	
		0.26	0.15	0.20	2.00	1.00	3.70		1.19	
5891	D1 + D2 Na	4.23	3.35		2.70	3.70	0.70		1.40	6.24
		0.50	0.65		0.70	0.70			1.22	
6015	Mn I	1.50			0.95				1.50	
		0.30			0.90				2.60	
6161	Ca I (+ Fe I)				3.50			1.61	1.30	
					3.00		2.75	1.50	1.49	
6250	TiO		3.46		1.72	2.75	2.00		2.11	
			1.40		0.20	2.00			0.76	
6563	Hα		4.59							
			1.40							
6820	CaH	3.66								
		1.30								

[a] Quoted by Wilson and Penston (1979).

TABLE II

Observed colours for the 6.3 arc sec central regions. More details in Dottori (1979).

Object	V	$(B-V)$	$(U-B)$
NGC 5530	12.39	1.18	1.17
5643	15.38	0.42	0.33
6699	14.08	0.87	0.23
1097	13.79	1.16	0.09
2997	14.81	0.61	−0.18
5236	12.36	0.41	−0.38
1566	13.76	0.96	0.25
3783	13.85	0.53	−0.98
IC 4329A	14.71	1.01	0.47
	±0.03	±0.04	±0.05

We define as the best solution that minimizing the addition of the squares of the differences between the computed and the measured equivalent width:

$$\mathfrak{F}(X_{\lambda_0,i}) = \sum_{l=1}^{15} p_l \quad W_l - \sum_{l=1}^{25} X_{\lambda_0,i} W \frac{F_{l,i}/F_{\lambda_0,i}}{\sum_{d=1}^{25} X_{\lambda_0,i} F_{l,i}/F_{\lambda_0,j}} , \qquad (1)$$

where $X_{\lambda_0,i}$, the unknown, is the percentual contribution of group i to the nuclear continuum at wavelength λ_0; $F_{\lambda,i}$, flux of a star of type i in the continuum light of wavelength λ; $W_{l,i}$, equivalent width of the absorption line l in a star of type i; W_l, equivalent width of the line l in the studied nucleus; P_l, the weight of the line l; $\mathfrak{F}(X_{\lambda_0,i})$, function to be minimized.

(b) The present proportion of stars of a given MS spectral type to any other later MS one, must be smaller than or equal to the primordial proportion provided by the IMF.

$$\frac{X_{\lambda,i}}{f_{\lambda,i}} \frac{f_{\lambda,\mathrm{M5V}}}{X_{\lambda,\mathrm{M5V}}} - S_{i,\mathrm{M5V}} \leq 0 \quad (i = \mathrm{O5V}, \ldots, \mathrm{M0V}) , \qquad (3)$$

where $S_{i,\mathrm{M5V}}$, relative number of stars of type i to M5V in the IMF.

We addopt for the initial vector the Salpeter's IMF:

$$N(M_i) \propto M_i^{-(1+x)} ,$$

where the slope x is a free parameter with initial value set at 1.45.

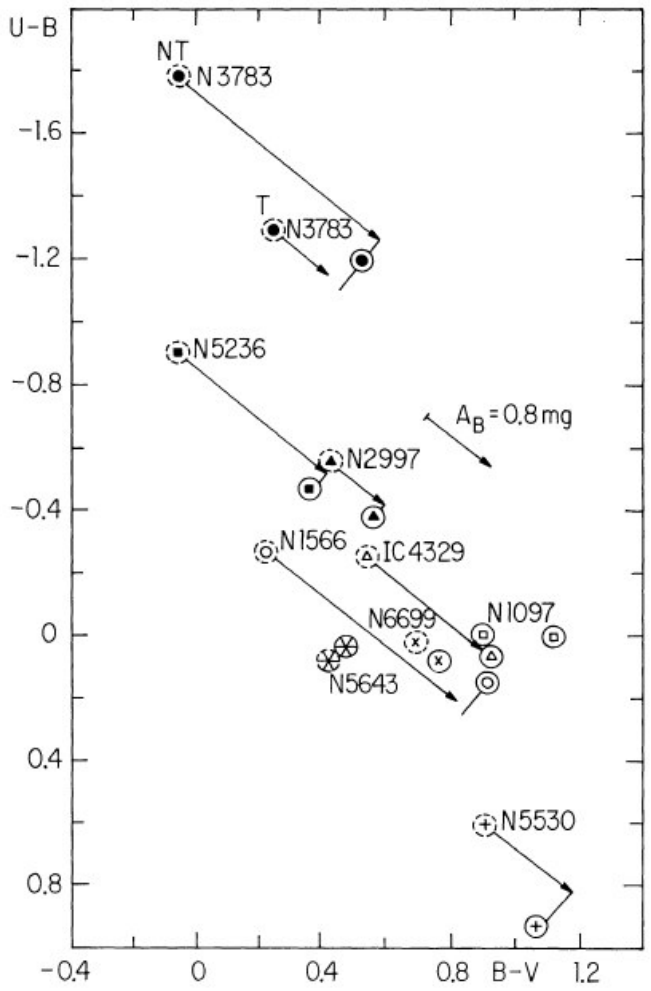

Fig. 1. $(U - B)$ vs $(B - V)$ diagram showing the observed colours for the 6.3 arc sec central region for each galaxy, de-reddened by extranuclear absorption (full circles) and the theoretical colours consistent with the reddening arrow. The length of the arrow binding model and observation correspond to the predicted internal absorption.

TABLE III

Relative number of stars, obtained from the synthesis assuming an arbitrary mass of $10^{10} M_{\odot}$ for the nuclei

Stellar type	Stellar composition										
N5530	N5643	N6699	N1097	N2997	N5236	N1566	N1566	N3783	N3783	4329A	
O5V	0	0	0	0	0	0	0	0	0	0	0
B0V	0	0	0	0	0	0	0	0.302E+05	0.691E+05	0	0
B5V	0	0.851E+06	0	0	0	0.106E+07	0.103E+07	0.101E+07	0.876E+06	0.968E+06	0.659E+06
A0V	0	0.439E+07	0.485E+05	0	0.593E+07	0.598E+07	0.607E+07	0.521E+07	0.449E+07	0.543E+07	0.370E+07
A5V	0.131E+08	0.126E+08	0.123E+05	0.111E+08	0.176E+08	0.163E+08	0.165E+08	0.150E+08	0.129E+08	0.148E+08	0.101E+08
F0V	0.221E+08	0.217E+08	0.732E+08	0.188E+08	0.272E+08	0.266E+08	0.270E+08	0.256E+08	0.221E+08	0.241E+08	0.165E+08
F5V	0.403E+08	0.429E+08	0.147E+09	0.339E+08	0.520E+08	0.532E+08	0.542E+08	0.507E+08	0.439E+08	0.484E+08	0.330E+08
G0V	0.700E+08	0.781E+08	0.209E+09	0.600E+08	0.956E+08	0.966E+08	0.980E+08	0.914E+08	0.808E+08	0.897E+08	0.605E+08
G5V	0.107E+09	0.919E+08	0.313E+09	0.918E+08	0.144E+09	0.146E+09	0.148E+09	0.111E+09	0.944E+08	0.133E+09	0.897E+08
K0V	0.156E+09	0.140E+09	0.512E+09	0.134E+09	0.212E+09	0.193E+09	0.176E+09	0.170E+09	0.145E+09	0.187E+09	0.104E+09
K5V	0.208E+09	0.197E+09	0.730E+09	0.179E+09	0.262E+09	0.245E+09	0.235E+09	0.238E+09	0.209E+09	0.229E+09	0.144E+09
M0V	0.449E+09	0.667E+09	0.186E+09	0.477E+09	0.547E+09	0.535E+09	0.543E+09	0.558E+09	0.476E+09	0.518E+09	0.335E+09
M5V	0.320E+10	0.403E+10	0.121E+10	0.216E+11	0.384E+10	0.420E+10	0.427E+10	0.466E+10	0.401E+10	0.376E+10	0.336E+10
F0III	0.433E+07	0.464E+06	0.204E+06	0.320E+07	0.196E+07	0.116E+07	0.107E+07	0.549E+06	0.473E+06	0.180E+07	0.208E+07
F5III	0.360E+07	0.386E+06	0.170E+06	0.266E+07	0.163E+07	0.960E+06	0.893E+06	0.456E+06	0.393E+06	0.150E+07	0.173E+07
G0III	0.300E+07	0.322E+06	0.142E+06	0.222E+07	0.136E+07	0.800E+06	0.745E+06	0.380E+06	0.328E+06	0.125E+07	0.144E+07
G5III	0.209E+07	0.225E+06	0.987E+05	0.154E+07	0.947E+06	0.558E+06	0.519E+06	0.265E+06	0.228E+06	0.870E+06	0.101E+07
K0III	0.177E+07	0.189E+06	0.832E+05	0.130E+07	0.799E+06	0.470E+06	0.438E+06	0.224E+06	0.297E+07	0.733E+06	0.847E+06
K5III	0.933E+06	0.100E+06	0.433E+05	0.688E+06	0.422E+06	0.249E+06	0.231E+06	0.118E+06	0.166E+07	0.388E+06	0.448E+06
M0III	0.775E+06	0.832E+05	0.360E+05	0.572E+06	0.351E+06	0.207E+06	0.192E+05	0.982E+05	0.847E+05	0.322E+06	0.372E+05
M5III	0.530E+06	0.569E+05	0.246E+05	0.391E+06	0.241E+06	0.141E+06	0.131E+05	0.671E+05	0.579E+05	0.220E+06	0.254E+06
SMR											
K0III	0.177E+07	0.883E+06	0.820E+05	0.130E+07	0.799E+06	0.470E+06	0.437E+06	0.223E+06	0.193E+06	0.733E+06	0.847E+06
K5III	0.933E+06	0.106E+06	0.436E+05	0.688E+06	0.422E+06	0.249E+06	0.231E+07	0.118E+06	0.102E+06	0.388E+06	0.448E+06
M0III	0.775E+06	0.832E+05	0.360E+05	0.184E+07	0.351E+06	0.207E+06	0.192E+05	0.982E+05	0.847E+05	0.322E+06	0.372E+05
M5III	0.530E+06	0.133E+05	0.246E+05	0.391E+06	0.240E+06	0.141E+06	0.131E+07	0.671E+05	0.579E+05	0.220E+06	0.254E+05

(a) Two other cycles of star formation with TOPs between G0V and M0V.

(b) The relative intensity of the burst with TOP around G0V is approximately the same for all the objects, while the oldest one is very intense for NGC 5643, 1097 and IC 4329A.

NGC 5530 present four cycles, among them one very strong at F0V. In NGC 5643 arise also four TOPs, showing the youngest of them trace of B5V stars.

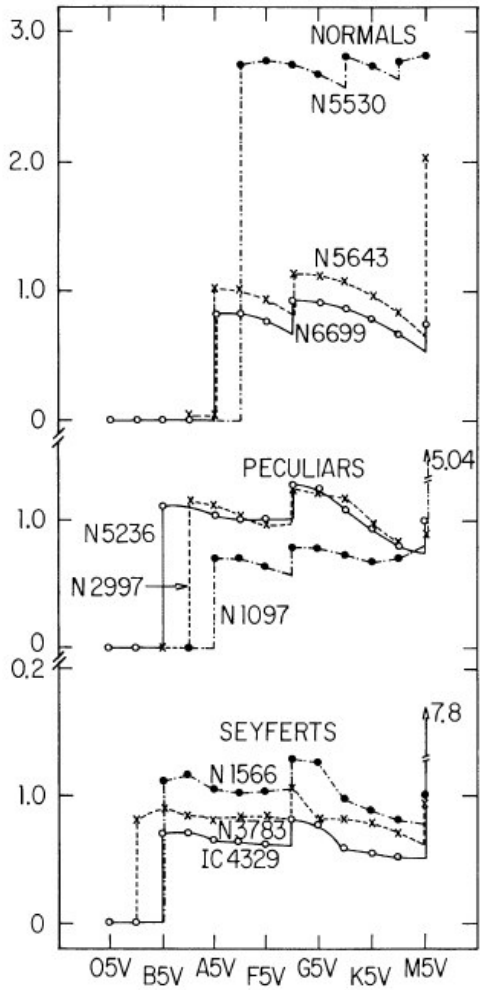

Fig. 2. Ratio Π_i/XS_i (see Section 3.4) vs MS spectral type. Jumps indicate the TOPs corresponding to cycles of star formation. Departure of Π_i from constancy between successive TOPs indicate departure of the IMF from the Salpeter's $x = 1.45$.

TABLE V

Equivalent width derived theoretically for the lines used in the process of synthesis

Line	Synthetic equivalent width											
	N5530	N5643	N5643	N6699	N1097	N2997	N5236	N1566	N1566	N3783	N3783	N4329A
Fe I (3632 Å)	1.6	1.9	0.7	2.2	2.1	1.7	1.2	1.2	0.6	0.8	1.2	1.4
Mg + H (3832 Å)	8.6	8.6	3.8	12.7	10.8	6.1	4.5	4.4	2.9	4.6	4.8	6.3
Hg + Fe I (3889 Å)	6.5	8.1	7.8	6.9	8.1	9.2	9.0	9.1	7.5	7.8	8.1	8.3
K Ca II (3933 Å)	7.0	8.1	4.5	11.1	8.5	7.0	5.5	5.6	4.1	4.7	5.2	5.7
H Ca II + Hg (3970 Å)	10.2	12.5	11.1	11.2	12.6	13.3	12.1	12.2	9.6	10.0	11.0	11.3
H (4101 Å)	6.4	8.4	8.4	5.5	8.1	10.3	10.1	10.3	8.2	8.2	8.9	9.0
G band (4300 Å)	3.8	4.0	2.2	5.9	5.0	3.2	2.4	2.4	1.7	2.4	2.5	3.5
Fe I (4384 Å)	5.5	7.3	7.6	5.0	6.6	9.0	9.0	9.2	7.8	7.6	7.9	7.4
Ca I + Fe I (4440 Å)	0.9	1.0	0.6	1.3	1.2	0.8	0.6	0.6	0.4	0.6	0.6	0.8
Ca I + Fe I (4592 Å)	0.4	0.6	0.6	0.5	1.4	0.3	0.2	0.2	0.2	0.1	0.3	1.7
Swan band (4658 Å)	1.6	2.1	1.5	1.7	4.5	1.2	0.9	0.9	0.6	0.8	1.0	4.9
Mg I (5174 Å)	2.7	3.2	3.0	3.6	5.0	2.4	1.9	1.9	1.4	1.8	2.0	4.4
Fe I + Ca I (5270 Å)	1.2	1.3	1.2	1.8	1.6	1.1	0.9	0.9	0.7	0.8	1.0	1.3
MaD (5890 Å)	2.8	3.5	3.6	3.2	5.9	2.5	2.1	2.0	1.6	1.8	2.2	6.0
Ca I + (Fe I) (6161 Å)	0.5	0.5	0.4	0.6	0.7	0.5	0.4	0.4	0.3	0.4	0.4	0.6

A base of star clusters for stellar population synthesis*

E. Bica and D. Alloin

Observatoire de Paris, Section de Meudon LAM, F-92195 Meudon Principal Cedex, France

Received May 5, 1985; accepted January 16, 1986

Astron. Astrophys. 162, 21–31 (1986)

Table 1. Characteristics of the clusters' sample

NAME NGC	AGE 10^7 yrs	$[Z/Z_\odot]$	E(B−V)	AREA 'x'	EXP min	SOURCES
			Small Magellanic Cloud			
121	1200±300	−1.24±0.3	0.03[a]	1x1	60	[3], [5], [6], [10], [19]
330	1.5±0.6	−1.4 ±0.4	"	1x1	20	[3], [6], [7], [15], [19], [32]
419	200±100	−1.2 ±0.3	"	1x1	40	[1], [5], [6], [7], [10], [19]
N 88	<0.2[b]	−0.95[c]	"	0.06x0.22	10	[19], [30], [31]
			Large Magellanic Cloud			
*1466	1400±300	−1.6 ±0.3	0.06[a]	1x0.5	50	[3], [10], [11], [19]
*1714 N4A	0.25±0.05[b]	−0.4[c]	"	1x0.5	10	[19], [31]
1783	300^{+200}_{-100}	−1.0 ±0.5	"	1x1	70	[5], [6], [7], [10], [19], [20]
*1831	30±10	−1.0 ±0.5	"	1x1	30	[5], [6], [7], [19], [22]
*1847	2.5±1.0	−0.25±0.4	"	1x1	26	[6], [19], [25]
*1856	10±3	−0.1 ±0.3	"	1x1	16	[6], [7], [19], [23]
1866	8.6±0.5	−1.2 ±0.2	"	{1x1 / 1x0.5	{20 / 20	[6], [7], [15], [16], [19]
1868	50±20	−1.1 ±0.2	"	1x0.5	40	[6], [18], [19]
*1895 N33	0.55±0.05[b]	−0.3[c]	"	1x0.5	30	[19]
1978	200^{+200}_{-100}	−0.8 ±0.4	"	1x0.7	50	[2], [5], [6], [10], [11], [19]
2004	0.8±0.1	−0.25±0.25	"	1x1	20	[6], [19], [20]
2070 30Dor	0.20±0.05	−0.5[c]	"	comp[d]	24	[17], [19], [24], [31]
*2100	1.0±0.2	−0.5 ±0.1	"	1x1	20	[3], [6], [19], [20]
2157	3±2	−0.6 ±0.3	"	1x0.5	20	[6], [15], [19]
2214	4±1	−1.2 ±0.2	"	1x1	30	[6], [7], [15], [19]
			Galactic Globular Clusters			
104 47TUC	1650±150	−0.70±0.15	0.08±0.04	3x3	12	[8], [9], [12], [13], [21]
362	"	−1.25±0.15	0.06±0.02	{1.5x1.5 / 1x0.5	{20 / 15	[4], [8], [9], [12], [13], [20]
1851	"	−1.3 ±0.2	0.09±0.02	1x0.5	10	[4], [8], [9], [12], [13]
1904 M79	"	−1.55±0.15	0.00±0.02	{1x0.5 / 1x1	{20 / 20	[4], [8], [9], [12], [13]
2808	"	−1.25±0.20	0.21±0.02	2x2	20	[8], [9], [12], [13]
4590 M68	"	−2.00±0.15	0.04±0.02	2x1	40	[4], [8], [9], [12], [13]
4833	"	−1.7 ±0.2	0.31±0.03	1.5x1.5	30	[4], [8], [9], [12], [13]
5024 M53	"	−1.85±0.15	0.01±0.02	2x0.5	30	[4], [8], [9], [12], [13]
5824	"	−1.8 ±0.2	0.12±0.02	1x0.5	10	[8], [9], [12], [13]
5927	"	−0.15±0.15	0.47±0.05	1x0.5	20	[8], [9], [12], [13], [21]
*5946	"	−1.5 ±0.2	0.61±0.07	0.5x0.5	19	[8], [9], [12], [13]
*6093 M80	"	−1.6 ±0.2	0.17±0.03	1x0.5	10	[8], [9], [12], [13]
*6139	"	−1.5 ±0.2	0.70±0.07	1x0.5	16	[8], [9], [12], [13]
6171 M107	"	−0.90±0.15	0.37±0.04	2x2	50	[4], [8], [9], [12], [13], [21]
*6287	"	−1.6 ±0.5	0.5 ±0.1	1x0.5	30	[8], [9], [12], [13]
*6293	"	−1.8 ±0.2	0.36±0.02	1x0.5	16	[8], [9], [12], [13]
*6304	"	−0.2 ±0.4	0.50±0.07	1x0.5	16	[8], [9], [12], [13]
*6316	"	−0.1 ±0.4	0.6 ±0.1	1x0.5	20	[8], [9], [12], [13]
*6356	"	−0.25±0.35	0.27±0.03	1x0.5	30	[8], [9], [12], [13]
*6388	"	−0.6 ±0.2	0.37±0.02	1.5x0.5	10	[8], [9], [12], [13]
*6401	"	−1.1 ±0.2	0.81±0.03	0.5x0.5	32	[8] [12], [13]
6402 M14	"	−1.1 ±0.3	0.55±0.06	2x2	50	[4], [8], [9], [12], [13]
6440	"	0.04±0.3	1.11±0.02	1x05	40	[8], [9], [12], [13]
*6453	"	−1.4 ±0.2	0.61±0.02	0.5x0.5	20	[8], [9], [12], [13]
*6517	"	−1.75±0.4	1.06±0.02	0.5x0.5	20	[8], [9], [12], [13]
*6528	"	−0.05±0.2	0.66±0.09	0.5x0.5	20	[8], [9], [12], [13]
6541	"	−1.65±0.25	0.12±0.05	2x0.5	20	[8], [9], [12], [13]
*6544	"	−1.1 ±0.4	0.72±0.08	0.5x0.5	20	[8], [9], [12], [13]
*6553	1650±150	0.1 ±0.4	0.79±0.09	1x0.5	50	[8], [9], [12], [13]
*6558	"	−1.3 ±0.2	0.40±0.15	0.5x0.5	20	[8], [9], [12], [13]

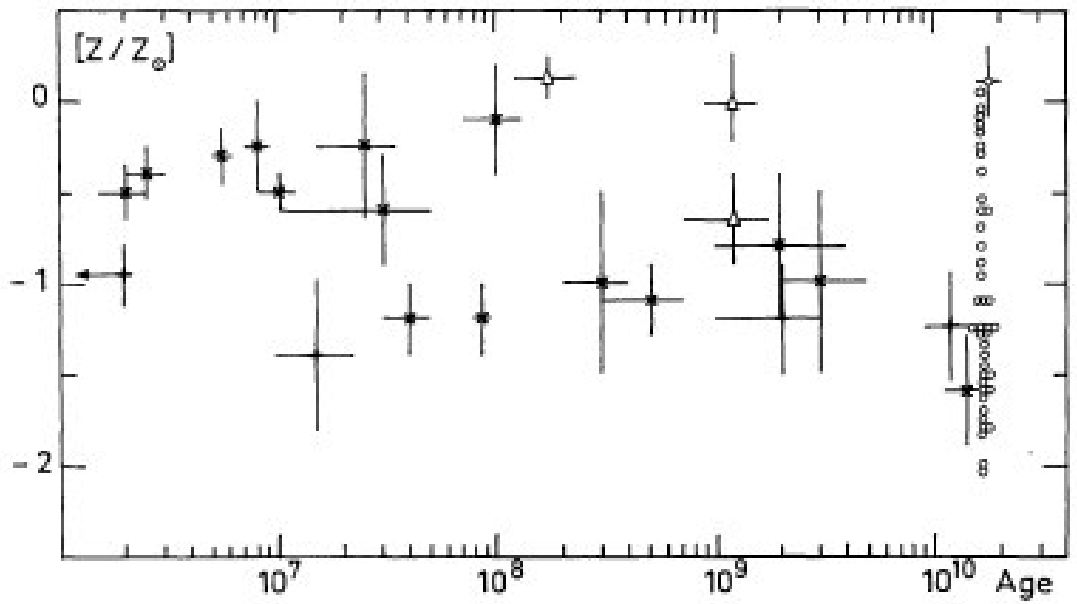

Fig. 1. Distribution of the cluster sample in the age, metallicity plane. For globular clusters, 1650 10^7 yr old, the typical error bar is indicated for one of the points only. Open triangles refer to Galactic open clusters (GOC); open circles to Galactic globular clusters (GGC); crosses and plus signs to the LMC and SMC clusters respectively

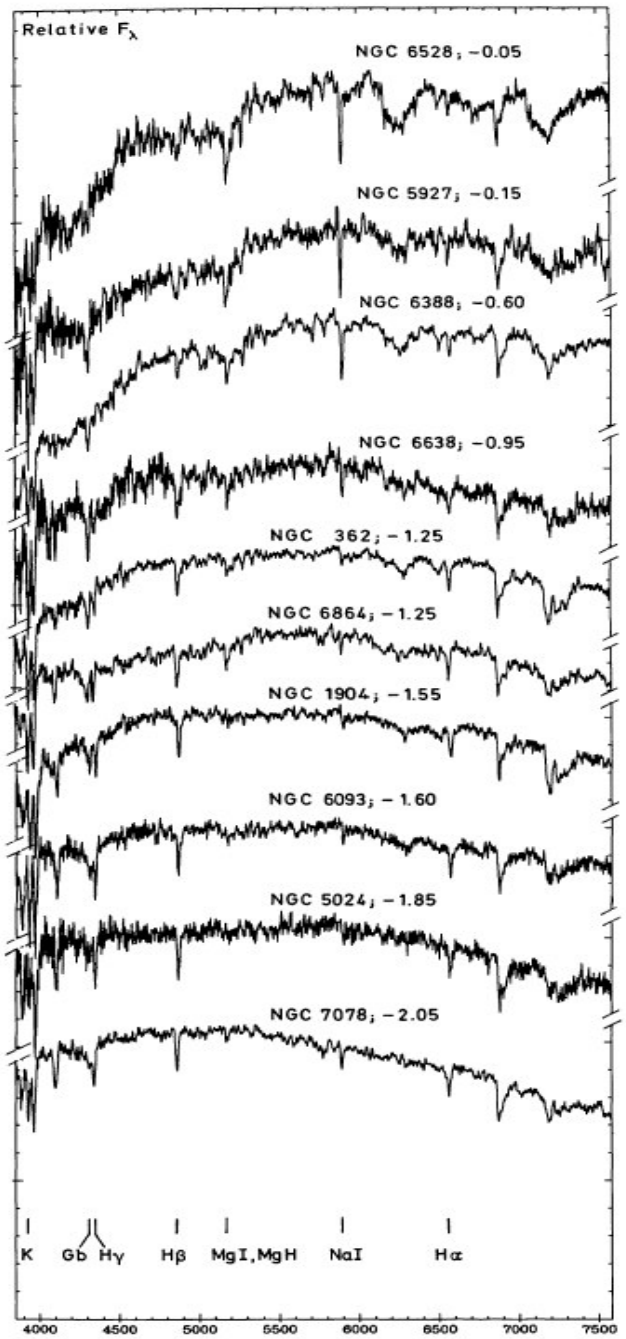

Fig. 2. The metallicity sequence for globular clusters. The spectra are corrected for foreground reddening and are normalized to

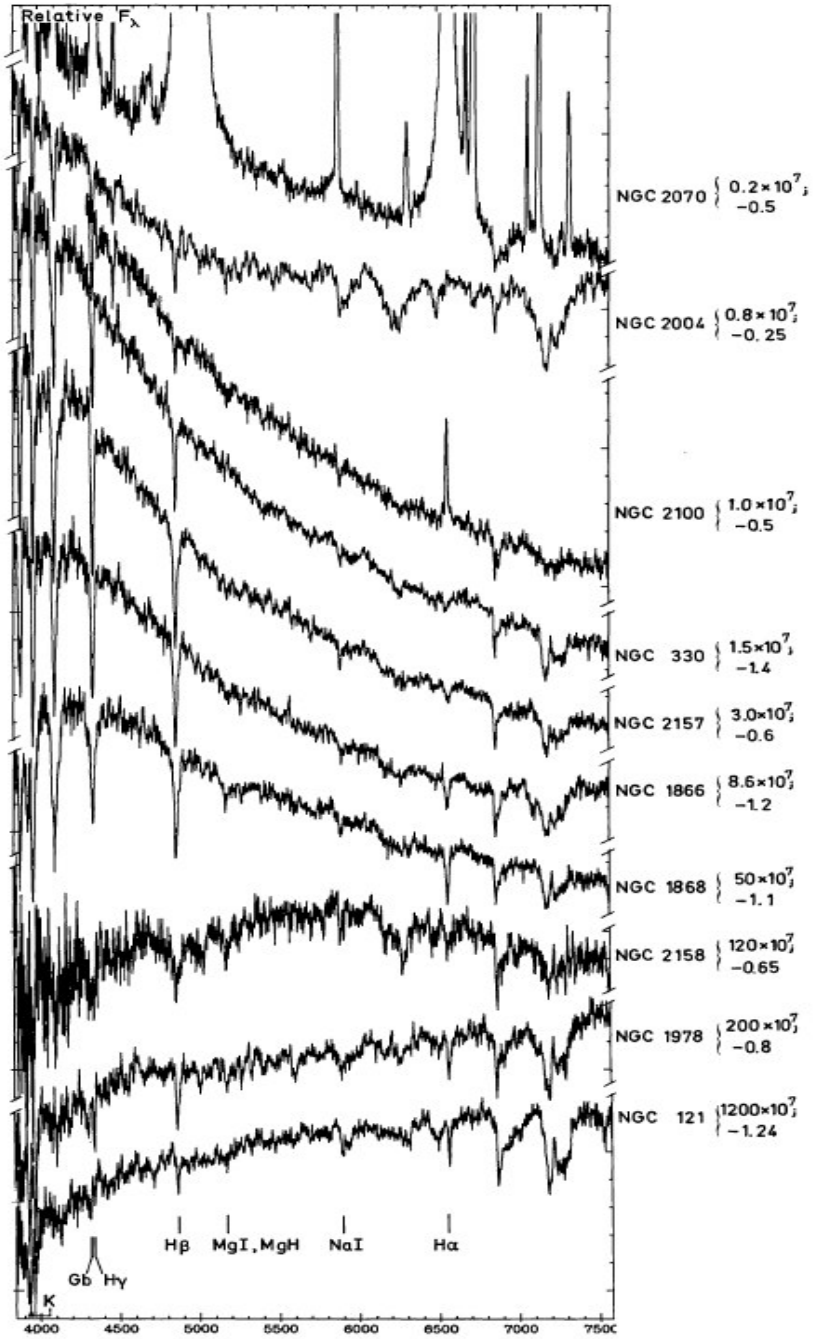

Fig. 3. The age sequence for young clusters. Reddening and normalization as in Fig. 2

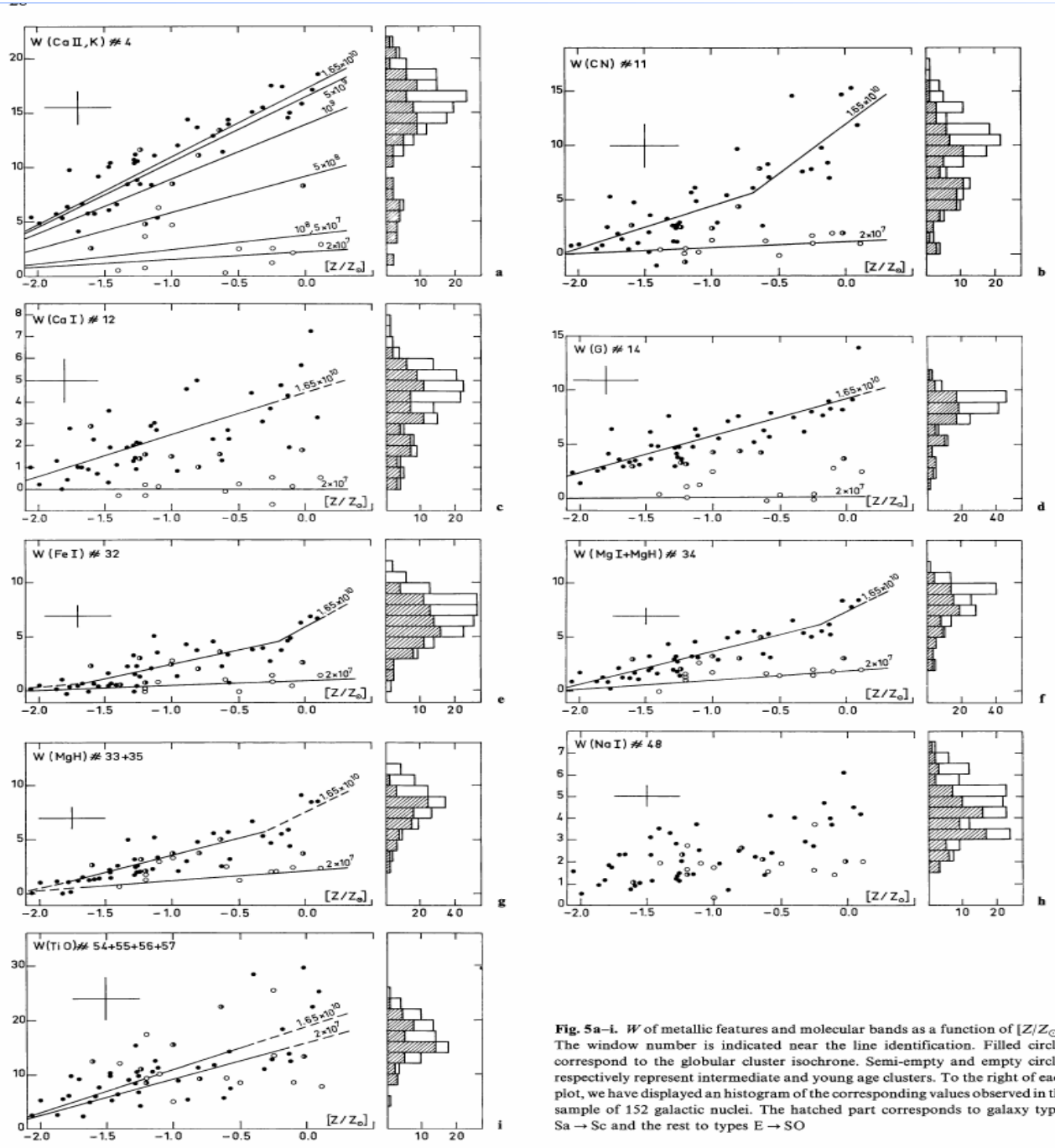

Fig. 5a–i. *W* of metallic features and molecular bands as a function of $[Z/Z_{\odot}]$. The window number is indicated near the line identification. Filled circles correspond to the globular cluster isochrone. Semi-empty and empty circles respectively represent intermediate and young age clusters. To the right of each plot, we have displayed an histogram of the corresponding values observed in the sample of 152 galactic nuclei. The hatched part corresponds to galaxy types Sa → Sc and the rest to types E → SO

Population synthesis in galactic nuclei using a library of star clusters ⋆

E. Bica
Observatoire de Paris, Section de Meudon, F-92195 Meudon Principal Cedex, France

Received June 15, accepted October 9, 1987

Astron. Astrophys. 195, 76–92 (1988)

Summary. Population syntheses for normal nuclei in E/S0 and spiral galaxies are derived using a library of star clusters. This method allows to determine the chemical enrichment and to date successive generations of star formation. Thus it is more than a simple population synthesis, providing for the first time a direct estimate of the chemical evolution in these nuclei. For the E/S0 groups following the normal metallicity vs luminosity relationship, the last generation of stars in the nucleus has reached a metallicity 4 times solar for $M_B = -22$ and 0.5 to 0.3 solar for $M_B = -18$. The bulk of the population is older than 10 Gyr but these galaxies have formed stars at least until look-back times of $\simeq 5$ Gyr. Some metallicity dispersion is detected within the nuclei: in the most metal rich group, around 10% of the optical flux arises from populations with metallicities lower than solar. For the relatively less numerous bluer E/S0 groups, younger age components are present, which we have been able to isolate and date. The red spiral groups also form a metallicity sequence which is related to the bulge luminosity, spanning metallicities from a factor 4 solar to solar. Finally, the groups of bluer spiral nuclei contain younger age components superimposed on an older population, which has reached at least the solar metallicity. The relative importance of the star formation bursts with respect to the older population is derived: in the bluest group, with NGC 5236 as a prototype, the population younger than $3\ 10^8$ yr amounts to 87% of the flux at 4000 Å and 57% at 9000 Å. The present method constitutes a powerful tool for the interpretation of composite spectra and will certainly have many applications in the study of large redshift galaxies.

Key words: galaxies: evolution of – galaxies: stellar content of – galaxies: general – galaxies: nuclei of

Population synthesis in galactic nuclei using a library of star clusters *

E. Bica

Observatoire de Paris, Section de Meudon, F-92195 Meudon Principal Cedex, France

Astron. Astrophys. 195, 76–92 (1988)

	Sa	Sb	Sc
Spectral group S1:			
$M<-22$	1	2	1
$-22<M<-21$	4	–	–
$M>-21$	1	–	–
Spectral group S2:			
$M<-22$	1	2	–
$-22<M<-21$	3	1	–
$M>-21$	4	–	–
Spectral group S3:			
$M<-22$	1	2	3
$-22<M<-21$	5	8	5
$M>-21$	4	2	–
Spectral group S4:			
$M<-22$	–	2	1
$-22<M<-21$	–	2	3
$M>-21$	1	1	4
Spectral group S5:			
$M<-22$	–	1	1
$-22<M<-21$	–	–	6
$M>-21$	–	1	–
Spectral group S6:			
$M<-22$	–	–	–
$-22<M<-21$	–	–	3
$M>-21$	–	–	2
Spectral group S7:			
$M<-22$	–	1	–
$-22<M<-21$	–	1	4
$M>-21$	–	–	1

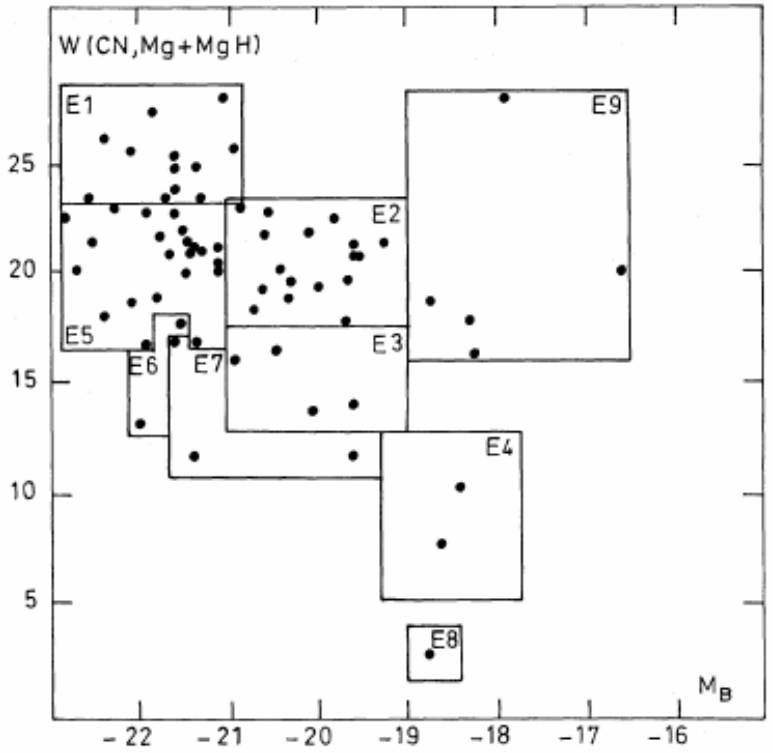

Fig. 1. Distribution of the E/S0 groups in a metal indicator vs absolute magnitude diagram

Table 3. Observed and computed properties and determination of the nuclear reddening

Group	W(K) 3933	W(CN) 4200	W(G) 4301	W(Mg I) 5175	W(Ca II) 8542	8662	Hβ 4861	Hγ 4340	Hδ 4102	Cont 4020	Cont 4570	Cont 7520	Cont 8700	$E(B-V)$ nucl.
E1	16.8	14.5	9.3	10.3	6.1	4.9	3.4	4.8	5.7	0.48	0.81	0.99	1.02	0.04
Temp.	18.7	15.0	10.3	9.2	6.4	5.7	3.8	5.1	4.8	0.49	0.76	0.98	0.99	
E2	17.2	10.9	9.2	9.5	6.2	5.3	3.6	5.1	4.9	0.53	0.82	1.00	1.01	0.05
Temp.	17.8	13.3	9.7	8.3	5.7	5.3	3.7	5.0	5.8	0.53	0.78	0.97	0.97	
E3	15.3	7.3	8.6	7.7	6.6	5.5	3.4	3.8	2.0	0.57	0.85	0.98	0.96	0.01
Temp.	14.9	9.4	8.2	6.3	5.0	4.6	3.6	4.9	4.4	0.60	0.81	0.94	0.92	
E4	13.7	3.4	6.8	6.3	5.2	4.7	ec	4.6	3.8	0.61	0.88	0.92	0.90	0.05
Temp.	12.0	5.7	6.5	5.5	4.4	3.9	3.7	4.6	4.6	0.65	0.84	0.92	0.89	
E5	15.8	10.6	8.7	9.6	5.4	4.5	3.4	4.0	3.8	0.50	0.81	1.00	0.99	0.05
Temp.	17.9	14.1	9.9	8.9	6.2	5.6	3.5	5.2	5.2	0.54	0.79	0.97	0.97	
E6	14.0	7.9	8.3	7.4	5.7	5.3	4.4	4.9	3.9	0.56	0.86	0.96	0.95	0.05
Temp.	15.5	10.9	8.5	7.2	5.3	4.9	4.1	5.3	5.1	0.65	0.84	0.93	0.91	
E7	12.5	6.2	6.5	7.2	5.5	5.0	4.7	4.9	5.6	0.67	0.95	0.86	0.83	0.01
Temp.	13.5	9.5	7.4	6.6	5.3	4.9	4.9	6.1	6.8	0.76	0.91	0.90	0.86	
E8	6.4	0.3	2.5	2.6	4.6	3.9	ec	6.6	9.2	1.21	1.19	0.79	0.72	0.04
Temp.	6.5	2.2	3.2	3.3	4.4	4.0	6.5	7.3	9.5	1.34	1.26	0.77	0.67	
S1	19.0	13.0	10.0	9.8	5.6	4.6	3.6	5.6	5.3	0.47	0.76	1.03	1.03	0.05
Temp.	18.6	14.7	10.2	9.0	6.3	5.6	3.7	5.1	4.6	0.50	0.77	0.98	0.99	
S2	16.4	10.4	8.8	9.2	5.9	4.6	3.7	3.9	4.1	0.50	0.79	1.00	1.02	0.05
Temp.	17.2	12.8	9.5	8.0	5.6	5.2	3.8	5.1	4.7	0.55	0.79	0.96	0.96	
S3	15.5	8.5	8.5	7.9	5.7	4.6	3.8	4.4	3.1	0.56	0.85	0.95	0.92	0.02
Temp.	15.3	10.8	8.5	7.1	5.3	4.9	3.9	5.2	4.9	0.61	0.82	0.94	0.92	
S4	13.1	6.2	7.3	6.3	6.2	4.7	4.2	5.4	4.2	0.59	0.80	1.02	0.98	0.04
Temp.	13.3	9.0	7.5	6.3	5.2	4.7	4.0	5.3	5.1	0.68	0.86	0.93	0.90	
S5	6.4	4.6	5.5	6.2	4.8	5.4	ec	ec	ec	0.67	0.87	0.98	0.94	0.07
Temp.	9.9	6.6	5.9	5.2	4.7	4.3	3.6	4.7	4.5	0.80	0.91	0.91	0.87	
S6	5.5	3.9	4.6	3.7	–	–	ec	ec	ec	0.86	0.95	0.95	–	0.06
Temp.	8.1	5.5	4.9	4.8	4.7	4.3	3.8	4.9	4.9	0.94	0.99	0.89	0.84	
S7	3.5	2.4	2.2	3.3	5.4	5.4	ec	ec	ec	1.34	1.27	0.76	0.63	0.01
Temp.	4.5	3.0	2.1	3.2	4.8	4.4	5.4	6.5	7.2	1.53	1.31	0.78	0.68	

Note to Table 3:
ec means that all galaxies in the group have the corresponding Balmer line contaminated by emission. Whenever part of the galaxies are contaminated, these were excluded from the mean

Table 4a–h. Percentage contributions at $\lambda = 5870$ Å: the chemical evolution for E/S0 groups

Table 4a
Group E1:

		Age (yr)							
		RHII	E7	5E7	E8	5E8	E9	5E9	Glob.
	+0.6						3	8	66
	+0.3								9
	0								5
$[Z/Z_\odot]$	−0.5								3
	−1.0								3
	−1.5								2
	−2.0								1

Table 4b
Group E2:

		Age (yr)							
		RHII	E7	5E7	E8	5E8	E9	5E9	Glob.
	+0.6								
	+0.3							11	74
	0								6
$[Z/Z_\odot]$	−0.5								4
	−1.0								3
	−1.5								1
	−2.0								1

Table 4c
Group E3:

		Age (yr)							
		RHII	E7	5E7	E8	5E8	E9	5E9	Glob.
	+0.6								
	+0.3								
	0							5	64
$[Z/Z_\odot]$	−0.5								14
	−1.0								11
	−1.5								4
	−2.0								2

Table 4d
Group E4:

		Age (yr)							
		RHII	E7	5E7	E8	5E8	E9	5E9	Glob.
	+0.6								
	+0.3								
	0								
$[Z/Z_\odot]$	−0.5						2	4	55
	−1.0								25
	−1.5								11
	−2.0								3

Table 4e
Group E5:

		Age (yr)							
		RHII	E7	5E7	E8	5E8	E9	5E9	Glob.
	+0.6						3	14	50
	+0.3								14
	0								6
$[Z/Z_\odot]$	−0.5								4
	−1.0								4
	−1.5								3
	−2.0								2

Table 4f
Group E6:

		Age (yr)							
		RHII	E7	5E7	E8	5E8	E9	5E9	Glob.
	+0.6								
	+0.3						7	17	40
	0								10
$[Z/Z_\odot]$	−0.5								9
	−1.0								7
	−1.5								6
	−2.0								4

E5 E6 E7 E8

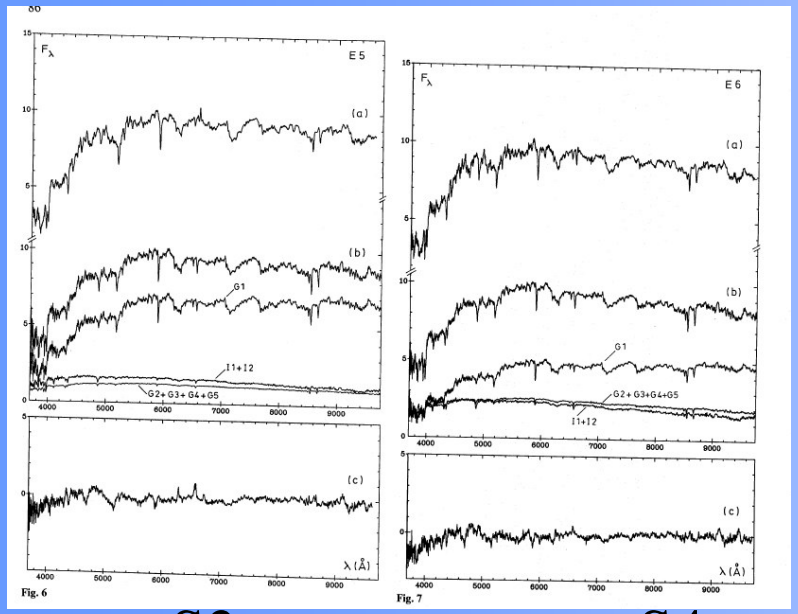

Fig. 6 Fig. 7

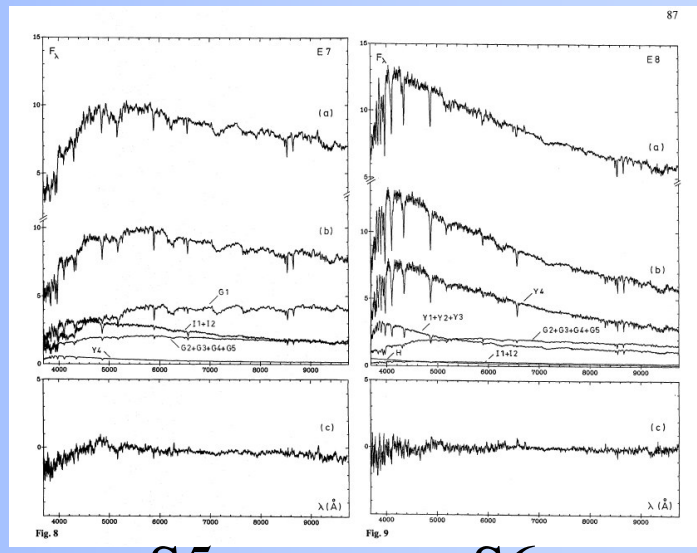

Fig. 8 Fig. 9

S3 S4 S5 S6

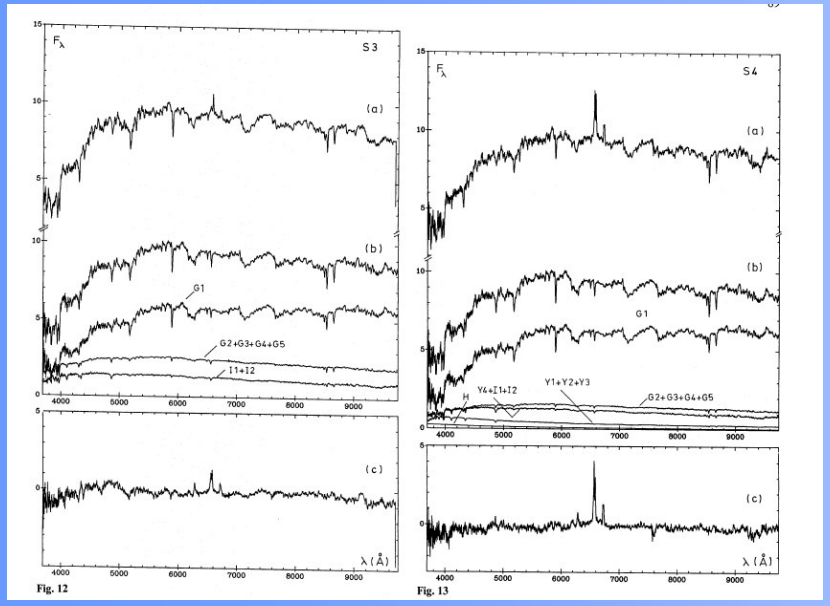

Fig. 12 Fig. 13

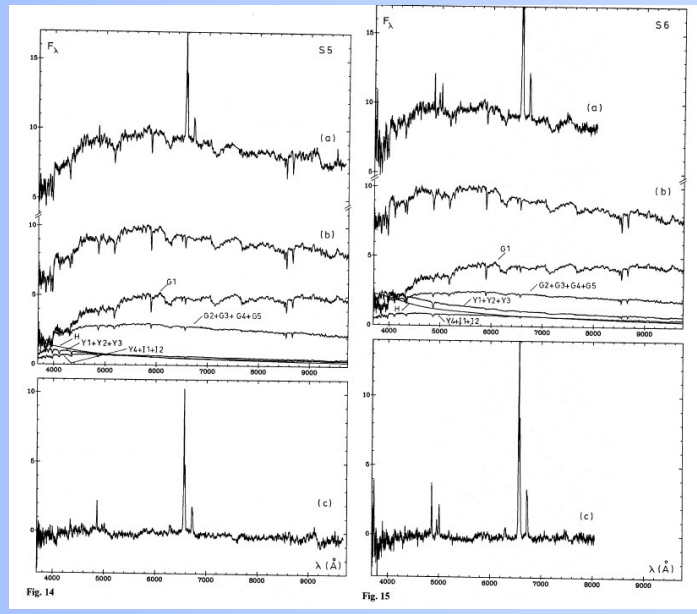

Fig. 14 Fig. 15

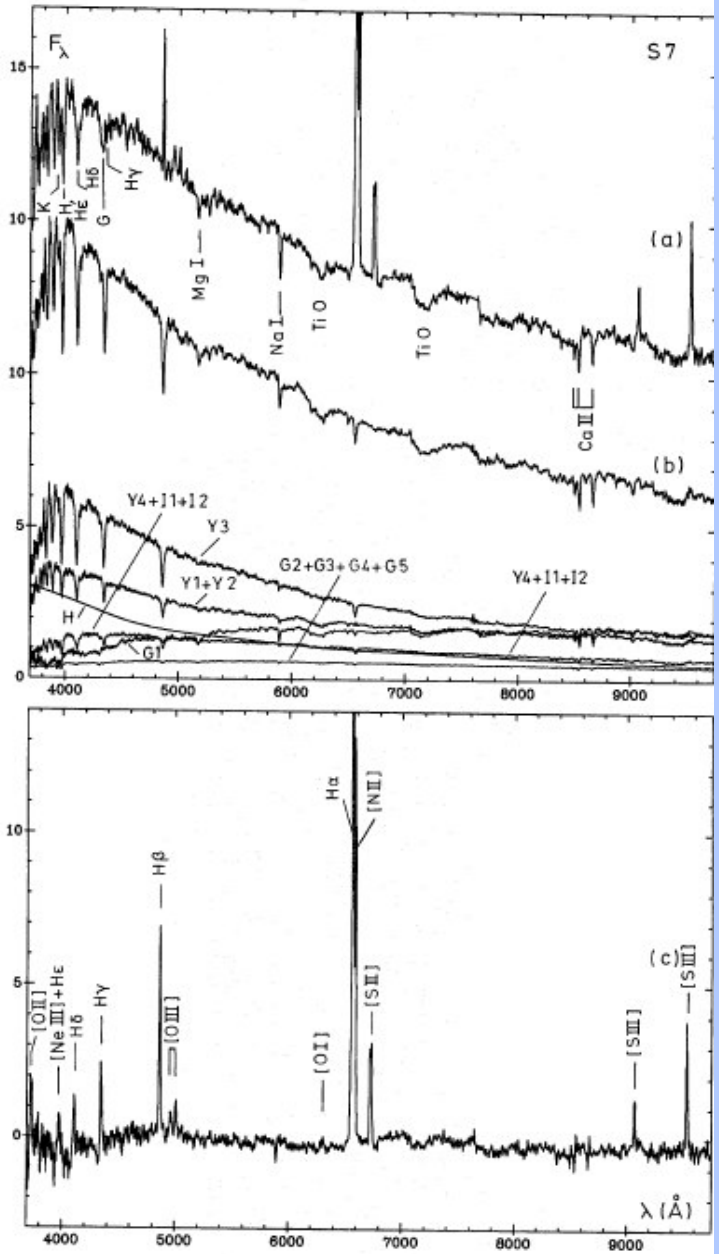
S7
(a)
(b)
(c)
K
H
Hε
Hδ
G
Hγ
Mg I
Na I
Ti O
Ti O
Ca II
Y4+I1+I2
Y3
G2+G3+G4+G5
Y1+Y2
Y4+I1+I2
H
G1
Hα
[NII]
Hβ
[SII]
[OI]
[OIII]
[NeIII]+Hε
Hδ
Hγ
[OII]
[SIII]
[SIII]
λ (Å)

Fig. 16

HST/ACS observations of the old and metal-poor Sagittarius dwarf irregular galaxy ⋆

Y. Momany[1], E. V. Held[2], I. Saviane[3], L. R. Bedin[1,4], M. Gullieuszik[1,2], M. Clemens[2], L. Rizzi[5], M. R. Rich[6], and K. Kuijken[7]

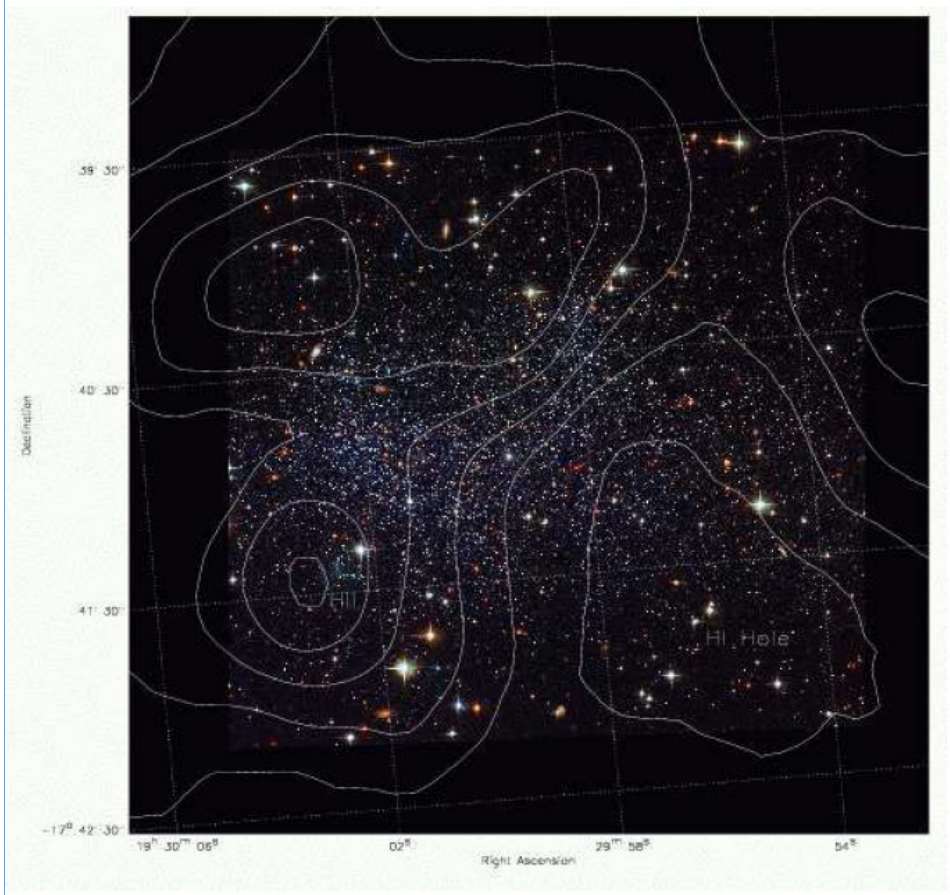

Fig. 2. True-color image of SagDIG derived from our ACS observations (see also http://heritage.stsci.edu/2004/31/index.html). A central, asymmetrical region of recent star formation, with faint extensions, is superimposed on a sheet of red giant stars belonging to the older stellar population of SagDIG. Superimposed are the H I column density contours from Young & Lo (1997). Also plotted are the locations of the H I hole and H II region.

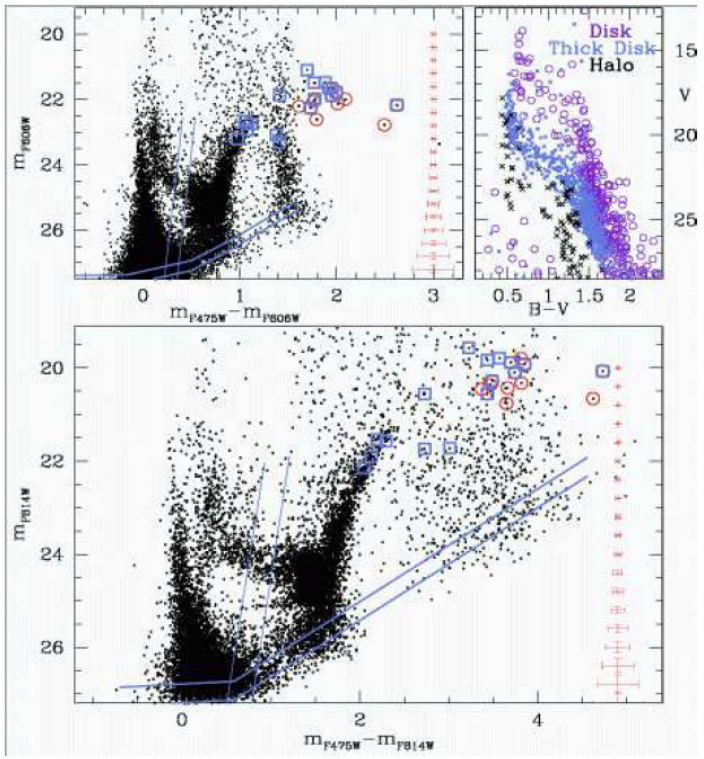

Fig. 3. HST/ACS color-magnitude diagrams of SagDIG. The *upper-left* panel shows the m_{F606W}, $(m_{F475W} - m_{F606W})$ diagram for stars with $|SHARP| < 0.3$. The *thick lines* represent the 80% and 50% completeness levels as derived from artificial stars experiments. Mean error bars from the same experiments are plotted as a function of m_{F606W}. The *open symbols* represent the carbon stars identified by Demers & Battinelli (2002; *open circles*) and Cook (1987; *open squares*). The *thin lines* delimit the approximate location of the instability strip on the CMD. The *upper-right* panel shows a synthetic V, $(B - V)$ diagram in the direction of SagDIG, calculated using the WEB interface of the Besançon Galactic model (Robin et al. 2003). Different symbols refer to the contributions of the Galactic thin disk (*open circles*), thick disk (*small squares*) and halo (*crosses*). The *lower* panel shows the m_{F814W}, $(m_{F475W} - m_{F814W})$ diagram.